Improved Group Robustness via Classifier Retraining on Independent Splits

Anonymous authors
Paper under double-blind review

Abstract

Deep neural networks learned by minimizing the average risk can achieve strong average performance. Still, their performance for a subgroup may degrade if the subgroup is underrepresented in the overall data population. Group distributionally robust optimization (Sagawa et al., 2020a), or group RDO in short, is a standard baseline for learning models with strong worst-group performance. We note that this method requires group labels for every example at training time and can be prone to overfitting, requiring strong regularization. Given a limited amount of group labels at training time, Just Train Twice (Liu et al., 2021), or JTT in short, is a two-stage method that infers a pseudo group label for every unlabeled example first, then applies group DRO based on the inferred group labels. The inference process is also sensitive to model selection. To mitigate overfitting, we propose a simple method based on the idea of classifier retraining on independent splits of the training data. We find that using a novel sample-splitting procedure achieves robust worst-group performance in the fine-tuning step. When evaluated on benchmark image and text classification tasks, our approach consistently reduces the requirement of group labels and hyperparameter search during training. Experimental results confirm that our approach performs favorably compared with existing methods when either group labels are available during training or are only available during validation.

1 Introduction

For many tasks, deep neural networks are often developed where the examples in test sets follow the same distribution as the training set. The performance of deep networks worsens when the test set distribution differs from the training set distribution. This problem has been studied by various literature in the name of out-of-distribution (OOD) generalization. This is crucial in safety-critical applications such as self-driving cars (Filos et al., 2020) and medical image classification (Oakden-Rayner et al., 2020). Tackling distribution shifts for out-of-distribution generalization is one of the most important problems for the real-world deployment of deep learning models.

A notable setting where distribution shifts occur is the group-shift setting, where different data groups may have a distribution shift (Sagawa et al., 2020a). In this setting, there are predefined attributes that divide the input space into different groups of interest. Here, the goal is to find a model that performs well across several predefined groups. Prior work has observed that deep networks learned by empirical risk minimization suffer from poor worst-group performance despite good average-group performance.

The difficulty with learning group robust deep networks can be attributed to the phenomenon of shortcut learning (Geirhos et al., 2020) or spurious correlation (Sagawa et al., 2020a; Arjovsky et al., 2019). Shortcut learning poses that minimizing the empirical risk favors models that discriminate based on simpler, spurious features of the data. However, one would like the learning algorithm to produce a model that uses features and correlations that perform well not only on the train distribution but also on all potential distributions that a task may generate, like that of a worst-group distribution.

In recent years, the group-shift setting has received considerable attention. Sagawa et al. (2020a) investigates distributional robust optimization (Duchi et al., 2021; Ben-Tal et al., 2013) in this setting and introduces

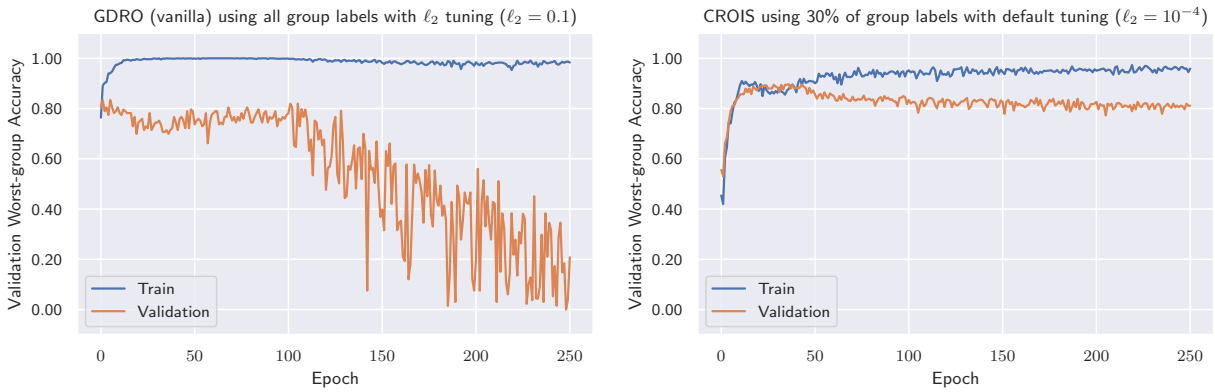

Figure 1: Worst-group learning curve on the Waterbird dataset between group DRO (**left**) and our method (**right**) from the setting in Section 4.2. In the left figure, the validation accuracy of group DRO becomes unstable as the number of epochs increases beyond 100 while the training accuracy remains close to 100%. Our approach instead uses 30% of the training data with group labels for fine-tuning the classification layer of a deep network that is obtained via minimizing the average risk using the rest of the training data without group labels (see also Algorithm 1). This allows our method to reuse features learned in the first stage while improving generalization compared with group DRO.

group distributionally robust optimization to optimize for the worst-group error directly. Since then, this approach has been the standard method for producing group-robust models, where it produces strong results that many follow-up works have used as a strong baseline (for example, see Liu et al. (2021); Nam et al. (2020); Zhang et al. (2022) and references therein). However, the worst-group error minimization problem is sensitive to small groups (Sagawa et al., 2020a) and requires group labels for all examples at training time.

Many works have considered ways to reduce the amount of group labels needed (Liu et al., 2021; Creager et al., 2021; Nam et al., 2022). These methods usually follow the framework of first inferring pseudo-group labels using a certain referenced model (pseudo-labeling) and then applying a group-robust algorithm like minimizing the worst-group loss on the pseudo-labeled data. While results for these methods have been promising, they usually introduce several more sensitive hyperparameters that can be expensive to tune. Our work aims to obtain group robust models using as few group labels as possible while alleviating the need to control model capacity.

Our Contributions. In this work, we propose a simple approach called *Classifier Retraining on Independent Splits* or CROIS in short. By replacing the pseudo-labeling phase to instead use group labels only for fitting the final classifier layer, our method achieves good robust performance without relying on a multitude of hyperparameters and large-scale tuning, which has been a growing concern in the community regarding reproducibility (Gulrajani and Lopez-Paz, 2021).

In short, our method takes advantage of the good features[1] learned by empirical risk minimization (Kang et al., 2019; Menon et al., 2021b) while overcoming the deficiency of its memorization behavior (Sagawa et al., 2020b) by utilizing the training data as two independent splits: one group-unlabeled split to train the feature extractor and one group-labeled split to retrain only the classifier with a robust algorithm like group DRO. We demonstrate through ablation studies that using independent splits is crucial for robust classifier retraining. Furthermore, our method's restriction of group DRO to only a low-capacity linear layer reduces group DRO's sensitivity towards model capacity as well as the amount of data needed for group DRO to generalize well (e.g., Figure 1 and Figure 3).

For various settings where group labels are only partially available during training (Section 4.1), our experimental results on standard datasets, including Waterbird, CelebA, MultiNLI, and CivilComments,

[1]We say *good features* (w.r.t. a certain task) to mean that there exists a linear classifier utilizing the deep network's features that perform well on our desired task, where features refer to the inputs to the deep network's final linear layer.

show improved performance over existing methods, including *Just Train Twice* (Liu et al., 2021) and *Spread Spurious Attribute* (Nam et al., 2022), despite minimal parameter tuning and no reliance on pseudo labeling. In another setting where more group labels are available (Section 4.2), even when using only a fraction of the available group labels, our competitive, robust performance against group DRO demonstrates our method's label efficiency. These results provide further evidence that deep networks contain good features on both image classification (Menon et al., 2021b) and natural language classification tasks. Finally, we provide a generalization bound for the worst-group loss in Section 5 to support the observation that we need a balanced split to obtain good group robustness.

2 Related Work

There are three main settings for the group-shift problem: (1) full availability of group labels, (2) limited availability of group labels, and (3) no availability of group labels, all referring to the training stage. Other related areas include domain generalization and long-tailed classification.

Fully-labeled group labels during training. Most methods here revolve around up-weighing minority groups, subsampling minority groups (Sagawa et al., 2020b), or performing group DRO (Sagawa et al., 2020a). Follow-up works include integrating data augmentation via generative model (Goel et al., 2020) or selective augmentation (Yao et al., 2022) to a robust training pipeline.

Partially-labeled group labels during training. In this setting, the approach of inferring more group labels for the group-unlabeled data remains the most popular. These pseudo-group labels are usually generated by training a referenced model that performs the labeling. For example, Liu et al. (2021) utilizes a low-capacity model that creates groups by labeling whether an example is correctly classified by the referenced model or not. Similarly, works like (Creager et al., 2021; Dagaev et al., 2021; Krueger et al., 2021; Nam et al., 2022) and (Nam et al., 2020) are variants of this approach of inferring pseudo group labels. These methods then proceed to use a group robust algorithm like group DRO (Sagawa et al., 2020a) or Invariant Risk Minimization (Arjovsky et al., 2019) to retrain new deep nets with the newly generated pseudo group labels.

No group labels during training. This setting removes the ability to validate knowledge of potential groups. This makes the problem more difficult as it is unclear which correlation to look for during training. Some theoretical works in this space include Hashimoto et al. (2018); Lahoti et al. (2020). Sohoni et al. (2020) proposes a popular empirical approach in this setting and has popularized the pseudo-labeling and retraining approach. This setting is related to domain generalization. Gulrajani and Lopez-Paz (2021) shows through mass-scale experiments that most out-of-distribution generalization methods do not improve over empirical risk minimization given the same amount of tuning and model selection criterion.

Long-tailed classification and evidences for good features. The long-tailed problem concerns certain classes having significantly fewer training examples than others (see, for example, Haixiang et al. (2017) or Zhang et al. (2021) for a survey). Some techniques from the long-tail literature, like Cao et al. (2019), have been applied to the group-shift setting to account for the group imbalances, as in Sagawa et al. (2020a).

Investigating the power of the features of deep nets has been of great interest in the long-tail setting (Liu et al., 2019; Menon et al., 2021a; Kang et al., 2019) as well as in the group-shift setting (Menon et al., 2021b). Kang et al. (2019) is one of the first works to provide extensive evidence for the hypothesis that deep nets contain good features via extensive experiments on several long-tailed vision datasets, where different strategies for obtaining feature extractors and fine-tuning the classification layer are examined. There, an ERM-trained feature extractor combined with a non-parametric method of rescaling[2] the classifier layer achieves (then) state-of-the-art results on all three datasets, showing evidence that the features of deep nets can be used to distinguish between rare and frequent classes. These insights are central to the development of our method.

Memorization in deep net training. It has now been well known of high capacity deep nets' ability to memorize training examples (Zhang et al., 2017). In the group-shift setting, this behavior has been investigated by Sagawa et al. (2020b), which provides empirical and theoretical justifications for deep nets'

[2]Rescaling each row of the linear classifier using the row's norm to some power. See Kang et al. (2019).

memorization behavior of minority groups' training examples. This behavior of memorizing minority examples has also been observed in the broader framework of data imbalances (Feldman and Zhang, 2020).

We would like to point out that, developed concurrently with our work, is a paper by Kirichenko et al. (2022), where the authors similarly discover that classifier retraining on independent splits via a similar procedure improves group robustness. While the main idea of retraining the classifier using independent splits is similar, Kirichenko et al. (2022) focuses more on exploring the features learned by deep networks. In contrast, our work focuses more on controlling model capacity for group DRO, where we limit its use to only the final linear layer. Thus, we believe that our method is of independent interest.

3 Method

This section describes the design of our method. First, we lay out the problem setup and the motivation behind this problem. Then, we describe our approach, which involves splitting the dataset into independent splits to conduct training features and classifiers separately.

3.1 Preliminaries

For a classification task $\mathcal{T}$ of predicting labels in $\mathcal{Y}$ from inputs in $\mathcal{X}$, we are given training examples $\{(x_i, y_i)\}_{i=1}^n$ that are drawn independent samples from some train distribution $\mathcal{D}_{\text{train}}$. In the domain generalization setting, we want good performance on some unknown test distribution $\mathcal{D}_{\text{test}}$ that is different but related to $\mathcal{D}_{\text{train}}$ through the task $\mathcal{T}$. More explicitly, we wish to find a classifier f from some hypothesis space $\mathcal{F}$ using $\mathcal{D}_{\text{train}}$ such that the classification error $L(f) = \mathbb{E}_{x,y\sim\mathcal{D}_{\text{test}}}[f(x) \neq y]$ of f w.r.t. $\mathcal{D}_{\text{test}}$ is low.

In the group-shift setting (Sagawa et al., 2020a), we further assume that associated with each data point x is an *attribute* $a(x)$ (some sub-property or statistics of x) from a set of possible attributes $\mathcal{A}$. These attributes, along with the labels, form the set of possible groups $\mathcal{G} = \mathcal{A} \times \mathcal{Y}$ that each example can take. We denote an input x's group label as $g(x) \in \mathcal{G}$. We then define the classification error of a predictor f (w.r.t. a fixed implicit distribution) restricted to a group $g \in \mathcal{G}$ to be $L_g(f) := \mathbb{E}_{x,y|g(x)=g}[f(x) \neq y]$. The notion of *worst-group error* upper bounds the error of f w.r.t. any group $L_{wg}(f) := \max_{g\in\mathcal{G}} L_g(f)$. Using this notation, the group-shift problem aims to discover a classifier in $\arg\min_{f\in\mathcal{F}}\{L_{wg}(f)\} = \arg\min_{f\in\mathcal{F}}\{\max_{g\in\mathcal{G}} L_g(f)\}$. We observe that the group-shift problem is just a special case of the domain generalization problem when $\mathcal{D}_{\text{test}}$ is the distribution consisting of only the points (x, y) with $g(x)$ being restricted to the worst-group of f in $\mathcal{G}$. Here, group distributional robust optimization solves this objective by performing a minimax optimization procedure that alternates between the model's weight and the relaxed weights of the groups.

Spurious correlations and memorization. As an example, consider the Waterbird dataset (Sagawa et al., 2020a), where it has been constructed by combining images of water/land birds from the CUB dataset (Welinder et al., 2010) with water/land backgrounds from the PLACE dataset (Zhou et al., 2017). The task is to distinguish whether an image of a bird is a waterbird or a land bird. Regarding our problem, the type of bird forms the labels $\mathcal{Y}$, and the backgrounds are set to be the attribute $\mathcal{A}$ for each type of bird. Altogether, these form four groups: $\mathcal{G} = \mathcal{Y} \times \mathcal{A} = \{\text{waterbird, landbird}\} \times \{\text{water, land}\}$.

This dataset is constructed so that the proportion of birds on matching backgrounds is significantly more than those of mismatched backgrounds. This is so that the backgrounds could be spuriously correlated with the labels, as predicting the background alone would achieve a high average accuracy w.r.t. the train distribution already. As expected, for models trained by empirical risk minimization, the groups with the highest error are the minority groups where the background mismatches the type of the bird, suggesting that the model is actually predicting using the background instead of the bird. Furthermore, the fact that these high-capacity models achieve *zero* training error leads to the conclusion that these models not only utilize spurious features like the background to make their predictions but also must have memorized the minority groups during its training process (Sagawa et al., 2020b). These problems are common when there is data imbalance in overparametrized networks (Feldman and Zhang, 2020; Li and Zhang, 2021) or when there is label noise (Ju et al., 2022). In the next section, we propose a method that attempts to circumvent these issues.

Algorithm 1 Classifier Retraining on Independent Splits (CROIS)

1: **Input:** Training data D_L with group labels and training data without group labels D_U. Classifier retraining algorithm $\mathcal{R}$ (default to group DRO). Optional splitting parameter p (default to 1).
2: *Obtain validation sets* by partitioning D_L into D'_L and $D_L^{(val)}$ and D_U into D'_U and $D_U^{(val)}$.
3: (Optional) *Add more unlabeled data* via split proportion p: Partition D'_L into two parts, D_1 and D_2 such that $|D_1| = (1-p) \cdot |D'_L|$ and $|D_2| = p \cdot |D'_L|$. Set $D'_L \leftarrow D_2$ and $D'_U \leftarrow D'_U \cup D_1$.
4: *Obtain the initial model* f by running empirical risk minimization on D'_U and selecting the best model in terms of average accuracy on $D_L^{(val)} \cup D_U^{(val)}$.
5: *Perform classifier retraining* $\mathcal{R}$ with feature extractor f on D'_L and then select the best model in terms of worst-group accuracy on $D_L^{(val)}$ as the final output.

3.2 Classifier retraining on independent splits

Algorithm 1 presents an outline for our main method: *Classifier Retraining On Independent Splits*, or *CROIS* in short. Given group-labeled data and group-unlabeled data, our method involves several steps:

1. Organize the data into one *group-labeled* split D'_L and one *group-unlabeled* split D'_U.
2. Obtain a feature extractor trained by empirical risk minimization with the group-unlabeled split D'_U.
3. Perform robust classifier retraining with the group-labeled split D'_L, where classifier retraining refers to fine-tuning the final linear layer of a deep network.

In the setting where group labels are limited (as in Section 4.1), $|D_L|$ is much smaller than $|D_U|$, and we do not need to set $p < 1$. There, we primarily concern with partitioning D_L into D'_L and $D_L^{(val)}$. On the other hand, when group labels are available for a large portion of the training dataset (as in Section 4.2) and $|D_U|$ is much smaller than $|D_L|$, the optional parameter p in step 3 controls the size of D'_U to obtain a feature extractor and the number of group labels D'_L actually used at train time.

Our method is motivated by empirical evidence that deep nets contain *good features*, as we shall soon discuss. On the other hand, deep nets' *weaknesses* involves memorizing examples and using spurious features. Our method is designed to alleviate these weaknesses while taking advantage of the good features of deep nets trained by minimizing the average risk over a large data population. As discussed in the related works section, there is extensive empirical evidence that deep nets trained by ERM contain features that can be used to distinguish between the minority classes from the majority classes in both the long-tailed setting and the group-shift setting. This suggests that a key to the group-shift problem is correcting the classifier layer, which forms the basis for the first phase of our method. The most efficient way to utilize data for fine-tuning the final layer was left open, and our work focuses on exploring this aspect in more depth.

Fine-tuning the classifier layer and utilizing group information. There is a range of possible strategies to utilize group labels. At one extreme, one can rescale using only minimal information, such as the group sizes, or at the extreme, one can maximally utilize group information by training the whole network with group DRO. Our work explores the space between these extremes by limiting the use of group labels to only fine-tune the final layer. Recall that in Kang et al. (2019), rescaling the classifier works best, whereas intuition suggests a data-dependent method like classifier retraining would work better. We hypothesize that this is related to the next issue of our discussion.

Memorization behavior of deep nets. As discussed in the related works section, there is strong evidence for deep nets memorizing training examples, which is often believed to be one of the main causes of poor robust performance. One way to circumvent memorization is to control the model's capacity by incorporating some combinations of high ℓ_2 regularization, early stopping, and other correctional parameters as has been done in Sagawa et al. (2020a). However, methods that are sensitive to different hyperparameter configurations with excessive tuning are not desirable, sometimes leading to reproducibility concerns (Gulrajani and Lopez-Paz, 2021). Our method, instead, does not require excessive tuning. It also extends to numerous settings depending on the availability of group labels.

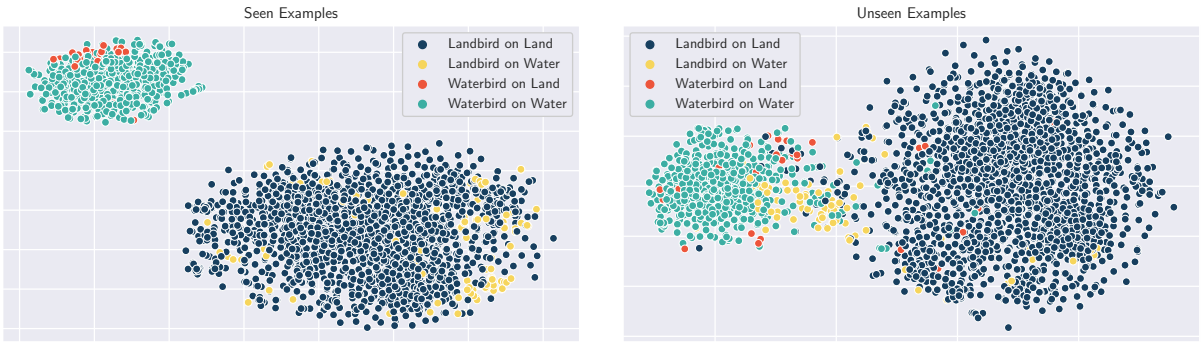

Figure 2: tSNE projection (Van der Maaten and Hinton, 2008) of the features of ResNet-50 on *seen* (**left**) versus *unseen* (**right**) examples from Waterbird.[3] The features of the minority groups (orange and yellow) from the *unseen examples* appear better separated from the majority groups than that of the seen examples. Using unseen examples plays a major role in our method's ability to improve worst-group performance via robust classifier retraining.

Tackling this memorization problem is crucial, and we achieve this using independent splits. As memorized examples' (i.e., already correctly classified) loss must be low, their gradients contain little useful information. Furthermore, the features of memorized examples might not represent their group during test time: Figure 2 presents a visualization of the features between seen versus unseen examples. Thus, combining this observation with the evidence for deep nets containing good features, our method performs robust classifier retraining on *unseen* examples (D'_L in Algorithm 1) in the hope of learning a classifier that utilizes features more representative of examples during test time. Our experimental results confirm these intuitions: the results from Table 3 show that robust classifier retraining without independent split indeed perform worse. Finally, as a side benefit, the independent split lends itself to theoretical analysis, which we provide in Section 5. This further supports the soundness of our method theoretically in addition to experimentally.

4 Experiments

We conduct experiments in two settings: (1) where group labels are only available from the validation split of the datasets (as in Liu et al. (2021); Nam et al. (2022)); and (2) when a fraction of group labels is available from the training split and all group labels are available from the validation split.

Setup. We use a similar setup to Liu et al. (2021) and Sagawa et al. (2020a). To demonstrate the ease of tuning of our method, unless noted otherwise (e.g. Table 2 and parameter p in Table 3), we *fix* the hyperparameters of both the empirical risk minimization (ERM) and the robust classifier retraining phase, reusing standard parameters for ERM (see Appendix A for full hyperparameters and model details). Further results of our method with tuned hyperparameters are presented in Section C of the Appendix.

Datasets. We experiment on four datasets:

- **Waterbird** (Sagawa et al., 2020a). Combining the bird images from the CUB dataset (Welinder et al., 2010) with water or land backgrounds from the PLACES dataset (Zhou et al., 2017), the task is to classify whether an image contains a *landbird* or a *waterbird* without confounding with the background. There are 4795 total training examples, whereas the minority group (*waterbird, land background*) has only 56 examples. We report the weighted test *average accuracy* due to the skewed nature of the val and test sets to be consistent with Sagawa et al. (2020a).

[3]Half of the data is used to obtain a feature extractor while the other half is used to obtain the features of the unseen examples.

Table 1: Experimental results for the setting when only group labels from the validation split are used. Results for JTT and SSA are taken from Liu et al. (2021) and Nam et al. (2022), respectively. The numbers in parentheses denote one standard deviation from the mean across 3 random seeds. See Table E in Appendix 18 for comparison with additional baselines.

	Waterbird		CelebA		MultiNLI		CivilComments	
Method	Avg Acc	Wg Acc	Avg Acc	Wg Acc	Avg Acc	Wg Acc	Avg Acc	Wg Acc
JTT	93.9	86.7	88.0	88.1	78.6	72.6	91.1	69.3
SSA	92.2 (0.87)	89.0 (0.55)	92.8 (0.11)	**89.8** (1.28)	79.9 (0.87)	76.6 (0.66)	88.2 (1.95)	69.9 (2.02)
CROIS (ours)	92.1 (0.29)	**90.9** (0.12)	91.6 (0.61)	88.5 (0.87)	81.4 (0.06)	**77.4** (1.21)	90.6 (0.20)	**70.3** (0.34)

- **CelebA** (Liu et al., 2015) is a popular image dataset of celebrity faces. The task is to classify the celebrity in the image is *blond* or *not blond*, with *male* or *not male* as the confounding attribute. There are 162770 total training examples, and the smallest group (*blond, male*) has 1387 examples.
- **MultiNLI** (Williams et al., 2017) is a natural language inference dataset for determining whether a sentence's hypothesis is *entailed* by, is *neutral* with, or *contradicts* its premise. The spurious attribute is the presence of negation words like *no, never*, or *nothing*. This task has 6 groups, with 206175 total training and 1521 in the minority group examples (*is entailed* and *contains negation*).
- **CivilComments-WILDS** (Borkan et al., 2019; Koh et al., 2021) is a natural language dataset where the task is to classify whether a sentence is *toxic* or *non-toxic*. There are 8 demographics – *male, female, white, black, LGBTQ, Muslim, Christian,* and *other religion*– forming 16 groups that *overlap*, because a comment can contain multiple demographics. Following Koh et al. (2021), we evaluate on all 16 groups but only use the attribute *black* along with the label in training. There is a total of 269038 training examples with 1045 minority examples from (*other religion*, *toxic*).

4.1 Result of using group labels from the validation split

Setup. In this section, we consider the setting where group labels D_L is available only from the standard validation split, where these group labels can be used for training (Nam et al., 2022) and/or model selection (Liu et al., 2021). Here, the training split is treated as the group-unlabeled set D_U. Most methods in this setting employ some pseudo-labeling approach to generate pseudo group labels that are then used to train a *new* network via a robust algorithm like group DRO. On the other hand, our method simply uses half of D_L for classifier retraining D'_L and the other half for model selection $D_L^{(val)}$ and does not rely on pseudo-labeling. Our method also reuses the initial model for the retraining phase, making our method closer to that of a single-phase procedure with additional fine-tuning.

Results. In Table 1, we compare our method against JTT (Liu et al., 2021) and SSA (Nam et al., 2022), where we report the mean and one standard deviation of the test average (*Avg Acc*) and worst-group Accuracy (*Wg Acc*) across 3 random seeds. There, our method outperforms JTT on all 4 datasets and SSA on 3 datasets using default parameters. Note that, unlike our method and SSA, JTT only uses available group labels for model selection. However, JTT requires training a large number of models across two phases, which can be expensive. Furthermore, JTT's model selection can be quite sensitive (see Section 5.4 of Liu et al. (2021)). SSA alleviates this problem of JTT by more efficiently utilizing group labels to infer pseudo-labeling. Finally, our method dispenses altogether with pseudo-labeling while still achieving competitive performance.

Discussion. We clarify the difference between JTT and our method. First, the initial phase of JTT is for *inferring* pseudo-group-labels for the group-unlabeled data. This phase requires careful hyperparameter tuning and capacity control using the group-labeled validation set to accurately produce pseudo group labels (as noted in section 5.4 of Liu et al. (2021)). On the other hand, our method trains a *single* model and simply retrains the last layer with any available group labels. Second, JTT's final performance is limited by group DRO's performance on the full network, which can worsen by mislabeled pseudo labels from the first phase.

Table 2: Worst-group test accuracy for partial group labels from the validation split. Results for SSA and JTT are taken from Table 3 of Nam et al. (2022). The standard deviation is reported based on three independent runs. See Table 19 in Appendix E for comparison with additional baselines.

% of group-labels from the validation split	CelebA			Waterbird		
	20%	10%	5%	20%	10%	5%
JTT (Liu et al., 2021)	81.1	81.1	82.2	84.0	86.9	76.0
SSA (Nam et al., 2022)	88.9	**90.0**	86.7	88.9	**88.9**	87.1
CROIS's Wg Acc	**89.6** (0.4)	87.6 (0.6)	**87.3** (1.0)	**90.4** (1.0)	**88.2** (0.9)	**87.8** (1.3)
CROIS's Avg Acc	90.8 (0.2)	91.6 (0.3)	87.8 (1.6)	92.4 (0.5)	93.0 (0.7)	88.7 (1.6)

Table 3: Comparison between our method CROIS and group DRO. NCRT refers to naive classifier retraining i.e., when an independent split is *not used* during the retraining phase. Results marked with † are taken from (Sagawa et al., 2020a). *For Waterbird, we omit the result for $p = 0.05$ due to the small dataset size and inability to sample any minority-group example for robust retraining.

	Waterbird		CelebA		MultiNLI		CivilComments	
Method	Avg Acc	Wg Acc	Avg Acc	Wg Acc	Avg Acc	Wg Acc	Avg Acc	Wg Acc
ERM	96.9	69.8	95.6	44.4	82.8	66.0	92.1	63.2
GDRO	93.2†	86.0†	91.8†	88.3†	81.4†	77.7†	89.6 (0.23)	70.5 (2.10)
CROIS' p – group-labeled fraction used for retraining (with $1-p$ unlabeled fraction for the ERM phase)								
0.05	*	*	91.9 (0.50)	88.9 (1.10)	81.8 (0.15)	73.8 (1.54)	90.8 (0.40)	63.3 (7.82)
0.10	95.4 (1.10)	83.5 (3.24)	91.3 (0.36)	90.3 (0.82)	80.8 (0.51)	75.3 (2.06)	89.5 (1.81)	68.7 (1.72)
0.30	90.8 (0.35)	**89.6** (1.15)	91.3 (0.44)	**90.6** (0.95)	80.0 (0.31)	**77.9 (0.17)**	89.7 (0.33)	68.6 (1.53)
0.50	90.4 (0.95)	89.5 (0.59)	91.9 (0.35)	88.2 (2.10)	79.8 (0.26)	74.4 (1.00)	89.5 (0.70)	**71.0** (1.50)
NCRT	96.5	75.2	93.9	69.2	82.3	67.9	90.3	67.6

In contrast, we demonstrate in Section 4.2 that, by limiting group DRO to only the last layer, our method is competitive to full group DRO even when using only a fraction of group labels and minimal tuning.

Compared with SSA (Nam et al., 2022), our method does not rely on pseudo labeling. In SSA, there is a pseudo-labeling phase along with a robust training phase using the inferred group labels. In the first phase, SSA trains a separate network that *predicts the group* rather than the class. By treating the pseudo-labeling problem as semi-supervised learning, SSA's pseudo-labeling capability is shown to improve upon JTT. Our results show that our method outperforms SSA on 3 out of 4 datasets while reusing default parameters.

Reducing validation split size. Following the setup in JTT (Liu et al., 2021) and SSA (Nam et al., 2022), we vary the size of the validation split (20%, 10% and 5% of the original) to test whether our results still hold in these settings. We consider both the Waterbird and CelebA datasets. Note that for this setting, our method must be additionally *tuned* to account for the increased difficulty of the reduced group-labels quantity. Nevertheless, the smaller examples quantity, along with just training the last layer, makes the extra tuning less expensive (details and setup in Section F). We present our results (along with error bars) in Table 2, where we find that our method outperforms JTT and SSA on various percentage levels.

4.2 Result of using partial training split group labels

Next, we consider the setting where group labels are available from both the training split and the validation split. In contrast to Section 4.1, the standard validation split is used *only* for model selection $D_L^{(val)}$ and not for classifier retraining D'_L here. We compare our method using some fraction of the training split's group

labels against group DRO using *all* the group labels. Again, we fix the parameters of our method to its standard empirical risk minimization parameter to demonstrate its ease of tuning (see Appendix A).

Setup. We study our method with different amounts of training group labels, determined by the parameter p. This means that $(1-p)$ fraction of the training split is used to obtain a feature extractor in the first phase D'_U (that uses no group label), and the rest p fraction of group labels are used for robust classifier retraining D'_L. This setup allows examining the trade-off between the quality of the feature extractor versus the amount of data available to perform classifier retraining. Additionally, to demonstrate the importance of retraining with *unseen* examples, we experiment with robust classifier retraining using the same data from the first phase, i.e., *without* independent splits – denoted as *NCRT* in the table.

The parameter p. In practice, we expect that $|D_L|$ is a lot smaller than $|D_U|$, as in Section 4.1. There, Table 2 suggests that reasonable robust performance can be achieved with a small fraction of group labels. In this setup, however, since the amount of group labels are abundant ($D_U = \emptyset$ and D_L is large), we treat p as a tune-able parameter that controls the size of D'_U and D'_L. Furthermore, using a p fraction of the available group labels simulates the process of obtaining group labels for a random fraction of the data if there is a budget constraint on group labels.

Results. In Table 3, our method outperforms group DRO on both image data sets and yields competitive performance to group DRO on the two text data sets when using only a fraction of group labels and reusing default hyperparameters. Our result implies that comparable or even better robust performance than group DRO can be obtained by collecting group labels for roughly 30% of the available training data (modulo validation). One exception is severe group imbalance cases, as in CivilComments (the minority group consists of only 0.4% of the dataset). There, a higher fraction of group-labeled data is beneficial to obtain more minority-group examples. Hence, a more efficient sampling method to include more minority examples (e.g., filter by labels first) would be beneficial in practice. Finally, the results for naive classifier retraining also show the importance of using an independent split for classifier retraining.[4]

Trade-off between feature extractor and amount of group-labeled data for robust retraining. From the results across the data sets, allocating more examples towards training the feature extractor (lower p) generally yields higher on-average accuracies. The worst-group error after classifier retraining has a more complex interaction with p, as it depends on both the quality of the feature extractor and the amount of group-labeled examples available to perform classifier retraining. While varying the proportion p in our experiments gives a rough estimate of this tradeoff, we hypothesize that the availability of minority group examples is the most important for obtaining a robust classifier. We further support this intuition with an ablation study in Section D.2 where removing non-minority examples has an insignificant impact on the final group-robust performance.

Alleviating group DRO's sensitivity towards model capacity. Group DRO's requirement for model capacity control via either ℓ_2 regularization or early stopping is well noted in the literature (Sagawa et al., 2020a). In Table 14, we compare group DRO and our method's sensitivity towards different ℓ_2 regularization. While our method's performance on Waterbird is relatively uniform, group DRO is more sensitive to different ℓ_2 settings on CelebA. When $\ell_2 = 1$ for CelebA, we see that group DRO fails altogether (see Figure 3). On the other hand, our method achieves consistent performance across different ℓ_2 settings. Our method controls the model capacity by limiting group DRO to only the last layer. This alleviates group DRO's tendency to overfit and simplifies parameter tuning (as in Figure 1 for Waterbird).

4.3 Ablation studies and discussions

Obtaining a good feature extractor. An ablation study on the effects of different validation accuracy and initial algorithms on the feature extractor's quality (measured by robust performance after classifier retraining) is presented in Section B. Similarly to previous works Kang et al. (2019), we find that empirical

[4]In Sagawa et al. (2020a), group adjustment (Cao et al., 2019) is observed to improve Waterbird's worst-group accuracy to 90.5%. We also notice an improvement when this is incorporated here and obtain a $90.3\% \pm 0.62$ test worst-group accuracy. We also observe that similarly to Sagawa et al. (2020a), the adjustment only works for Waterbird but not for CelebA nor MultiNLI.

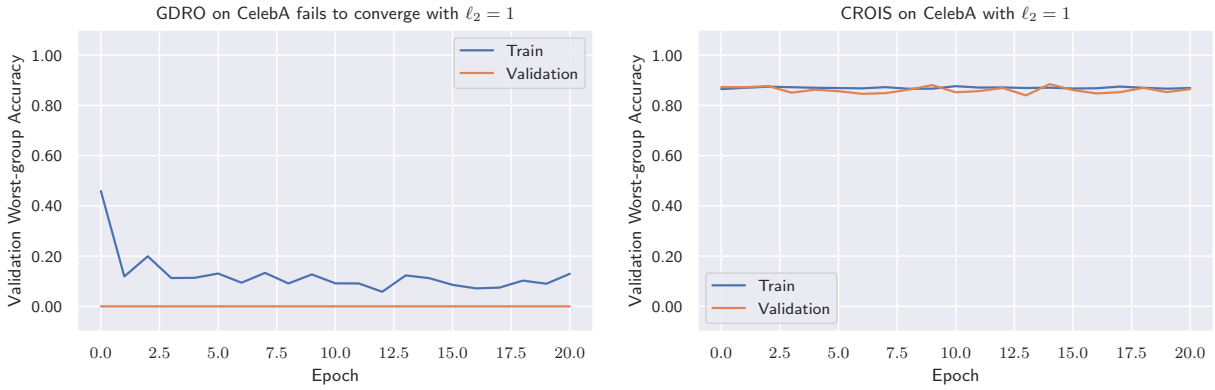

Figure 3: While group DRO often requires high ℓ_2 regularization to avoid overfitting, setting ℓ_2 too high might cause instability in group DRO's minimax optimization procedure (**left**).

Table 4: Comparison between reweighting, subsampling, and group DRO as classifier retraining algorithms on top of the same feature extractor ($p = 0.30$).

Retraining Method	Waterbird		CelebA		MultiNLI		CivilComments	
	Avg Acc	Wg Acc	Avg Acc	Wg Acc	Avg Acc	Wg Acc	Avg Acc	Wg Acc
Reweighting	95.2	87.1	92.1	85.0	78.9	67.0	88.3	56.4
Subsampling	95.8	81.1	91.6	86.1	78.6	64.0	91.8	59.3
GDRO	91.4	**90.2**	91.6	**90.4**	80.3	**78.0**	89.7	**69.1**

risk minimization provides the best features over reweighting or group DRO (both requiring group labels). We find that there's a positive correlation between validation average accuracy and features' quality. This then serves as a proxy for our method's model selection criterion in the first phase, significantly simplifying parameter tuning over other two-phase methods in the group-shift setting.

Group DRO is better than reweighting and subsampling for classifier retraining. Table 4 contains results on using different classifier-retraining methods. We observe that group DRO produces the best group-robust performance (since group DRO is designed for this setting, after all). Reweighting and subsampling seem to be effective on the vision datasets but fail to perform on the NLP datasets.

Table 5: Comparison between retraining with group DRO on the full network (*Full*) versus last layer retraining (*LL*).

GDRO $p = 0.30$	Waterbird		CelebA		MultiNLI		CivilComments	
	Avg Acc	Wg Acc	Avg Acc	Wg Acc	Avg Acc	Wg Acc	Avg Acc	Wg Acc
LL (CROIS)	91.4	**90.2**	91.6	**90.4**	80.3	**78.0**	89.7	69.1
Full	90.5	79.8	91.6	78.3	80.8	75.1	90.4	69.1

Classifier retraining outperforms full retraining with group DRO. Classifier retraining plays a central role in our method. In Table 5, we compare fine-tuning with group DRO on the full DNN versus just the last layer for an independent split of $p = 0.30$. We see that group DRO on the last layer is much better than full group DRO on most of the datasets (except CivilComments). However, the main difference is that while the last layer retraining requires little additional tuning, we must search for different regularization

strengths for group DRO when applied to the full network. our method can be shown to be quite robust to different parameter settings and regularization strengths (details in Appendix C.1).

Deep nets learned by minimizing the average risk contain good features. The positive result for our decoupled training procedure provides strong evidence for deep nets containing good features for the group-shift problem. While this is consistent with findings in the literature on vision datasets (Kang et al., 2019; Menon et al., 2021b), our work further provides some of the first evidence of this hypothesis in non-vision tasks, where the same result would not have been possible without independent split, as evident in the result for naive classifier retraining in Table 3.

Simplified model selection. The model selection criterion of picking the best average validation accuracy model simplifies hyperparameter tuning compared to other two-phase methods. This decision has been chosen mainly from the ablation experiments in Section B of the Appendix, where we observe that higher average validation accuracy generally suggests better features.

5 Theoretical Analysis via Generalization Bounds

In this section, we complement our empirical results with Radamacher-complexity-based generalization bounds for both phases of our method: one for the standard average loss for the deep net's feature extractor and another for the worst-group generalization bound for linear classifiers. These serve as an explanation for balancing the right proportion of samples within both phases, especially when the data imbalance between subgroups is large. We provide an upper bound on the worst-group loss that depends on the worst-group sample size. We then argue that the average generalization error lower bounds the worst-group generalization error, and a balanced splitting of the samples is beneficial to sufficiently control the worst-group error.

5.1 Generalization bound for average loss of deep nets

We first present the standard generalization bound for deep nets here. Given a dataset $S := \{(x_1, y_1), \ldots, (x_n, y_n)\}$, consider a function class $\mathcal{F}$ consists of L-layers feedforward neural network with ρ-Lipschitz activations along with the composed function class with the dataset $\mathcal{F}_{|S}$:

$$\mathcal{F} := \left\{ x \to \sigma_L \left(W_L \sigma_{L-1} \left(\cdots \sigma_1 \left(W_1 x \right) \cdots \right) \right) \mid \left\| W_i^T \right\|_{1,\infty} \leq B \right\}$$
$$\mathcal{F}_{|S} := \left\{ \left(\ell \left(f(x_1), y_1 \right), \ldots, \ell \left(f(x_n), y_n \right) \right) \mid f \in \mathcal{F} \right\}.$$

If we collect samples $x_1, \ldots, x_n$ into rows of $X \in \mathcal{X}^{n \times d}$ and if the activations σ_i are ρ-Lipschitz with $\sigma_i(0) = 0$, then we can show the following generalization bound for $\mathcal{F}$:

Theorem 1. *Suppose that $f \in [a, b]$ for all $f \in \mathcal{F}$ for some finite $a < b$. Then with probability at least $1 - \delta$*

$$\sup_{f \in \mathcal{F}} \mathbb{E}\left[f(Z) \right] - \frac{1}{n} \sum_{i=1}^{n} f(z_i) \leq \frac{2}{n} \left\| X \right\|_{2,\infty} (2\rho B)^L \sqrt{2 \ln (d)} + 3 (b - a) \sqrt{\frac{\ln (2/\delta)}{2n}}.$$

We defer the proof to Appendix G.

Convolution networks. We can view a simple convolution layer at depth l with kernels $K_1^{(l)}, \ldots, K_{k_l}^{(l)}$ as linear layers of Toeplitz matrices $W_1^{(l)}, \ldots, W_{k_l}^{(l)}$ representation the kernel. Then, for the $(1, \infty)$-norm for a convolution net with L layers, we scale with the size of the kernels rather than the dimension with standard linear layers:

$$\left\| W_j^{(l)} \right\|_{1,\infty} = \sum_i \left| K_{j,i}^{(l)} \right|.$$

With this view, we can apply the bound above to convolutional networks as in our experiments.

5.2 Worst group generalization bound for linear classifiers with logistic loss

In this section, we derive a generalization bound for the worst-group loss for linear classifiers. Suppose we are working with a binary classification problem with G groups, where for a sample $x \in \mathcal{X}$, we have that $g(x) \in [G]$. Consider the hypothesis class of linear classifiers with bounded norm i.e.

$$\mathcal{H} := \left\{ w \in \mathbb{R}^d \mid \|w\| \leq B \right\}.$$

Since the 0-1 loss $\ell(x, y) = 1[x \neq y]$ is a bit hard to work with, we instead consider the logistic loss

$$\ell(x, y) = \ln\left(1 + \exp\left(-yx\right)\right).$$

Hence, the function class along with our dataset $S := \{(x_1, y_1), \ldots, (x_n, y_n)\}$ we are considering for generalization is

$$\begin{aligned} \mathcal{F} &:= \left\{ (x, y) \to \ell\left(w^T x, y\right) \mid \|w\| \leq B \right\} \\ \mathcal{F}_{|S} &:= \left\{ \left(\ell\left(w^T x_1, y_1\right), \ldots, \ell\left(w^T x_n, y_n\right)\right) \mid \|w\| \leq B \right\}. \end{aligned}$$

We can further partition the dataset into its G groups: $S_1, S_2, \ldots, S_G$, where $S_i := \{(x, y) \in S \mid g(x) = i\}$ with sizes n_i each. Let

$$\hat{R}_i(f) := \frac{1}{n_i} \sum_{(x_j, y_j) \in S_i} \ell(f(x_j), y_j), \qquad R_i(f) := \mathbb{E}_{(X,Y)|g(X)=i}\left[\ell(f(X), Y)\right]$$

denote the empirical and population group loss of f. We can then show the following result:

Theorem 2. *If $\mathcal{F}$ is a class of bounded linear classifiers and l is the logistic loss, then for the binary classification with G groups, we have that with probability at least $1 - \delta$:*

$$\sup_{f \in \mathcal{F}} \underbrace{\max_{i \in G} R_i(f) - \hat{R}_i(f)}_{\textit{WG generalization error}} \leq \max_{i \in G} \frac{2}{n_i} B \cdot \left\| X^{(i)} \right\|_F + 3\left(\ln(2) + B\right) \sqrt{\frac{\ln\left(2G/\delta\right)}{2n_i}}.$$

We defer the proof to Appendix G.

5.3 Two stage training and data balancing

Note that since the worst-group loss upper bounds the average loss, the average loss is a natural lower bound on the worst-group loss. The generalization gap for the worst-group loss is not only influenced by its hypothesis class and the amount of data per group but it is also influenced indirectly by the lower bound given by the average loss for training the feature extractor. Hence, this suggests that the process of splitting the data into different proportions (via the parameter p) across two phases in our method is a means to trade-off between the worst-group and average loss generalization gap. Note that, as with most existing generalization bounds for deep networks, these bounds are most likely not informative and are just suggestions for algorithms design.

Empirical validation. We present some supporting empirical evidence in Table 6 where we show the worst-group loss and average loss generalization gap for various splitting proportions p for CelebA and Waterbird. The generalization gap shown below is selected from the best validation epoch. There, we obtain the best generalization when the splitting is "balanced" ($p = 0.30$) as in our other experiments.

6 Conclusion

In this paper, we propose classifier retraining on independent splits as a simple method to reduce the number of group annotations needed for improving worst-group performance as well as alleviate group DRO's

Table 6: Generalization gap between different splitting proportions of the training data for both phases.

	CelebA			Waterbird		
Splitting proportion p	0.1	0.3	0.5	0.1	0.3	0.5
Test worst-group loss	0.287	0.275	0.312	0.389	0.27	0.313
Train worst-group loss	0.249	0.269	0.236	0.183	0.25	0.295
Generalization gap	0.038	**0.006**	0.076	0.206	**0.02**	0.018

requirement for careful control of model capacity (Sagawa et al., 2020a). Our experimental results show the effectiveness of our method on four standard datasets across two settings and provide evidence that deep nets contain good features for the group-shift problem.

Future Work. The richness of deep net features can potentially be useful in solving the seemingly harder group-agnostic setting (where no group label is available) by allowing the practitioner to focus on obtaining a robust classifier given a feature extractor, where we have shown that reasonable robustness can be achieved with relatively few group-labels, which makes the problem seem closer in reach. On a broader note, while most work in representation learning focuses on producing good features (either with supervised, unsupervised, or self-supervised approaches), further examinations into different ways to perform classifier retraining in different settings (as in our work) could give a fuller picture to the features quality of different methods.

Broader Impact Statement. Worst group robustness is closely related to fairness in AI, where issues like biases of machine learning models are considered (Hardt et al., 2016; Ding et al., 2021). Our method seeks to improve the group robustness of deep learning models which is important as machine learning models are becoming more ubiquitous.

References

M. Arjovsky, L. Bottou, I. Gulrajani, and D. Lopez-Paz. Invariant risk minimization. *arXiv preprint arXiv:1907.02893*, 2019.

A. Ben-Tal, D. Den Hertog, A. De Waegenaere, B. Melenberg, and G. Rennen. Robust solutions of optimization problems affected by uncertain probabilities. *Management Science*, 59(2):341–357, 2013.

L. Biewald. Experiment tracking with weights and biases, 2020. URL `https://www.wandb.com/`. Software available from wandb.com.

D. Borkan, L. Dixon, J. Sorensen, N. Thain, and L. Vasserman. Nuanced metrics for measuring unintended bias with real data for text classification. In *Companion proceedings of the 2019 world wide web conference*, pages 491–500, 2019.

K. Cao, C. Wei, A. Gaidon, N. Arechiga, and T. Ma. Learning imbalanced datasets with label-distribution-aware margin loss. *Advances in Neural Information Processing Systems*, 32:1567–1578, 2019.

E. Creager, J.-H. Jacobsen, and R. Zemel. Environment inference for invariant learning. In *International Conference on Machine Learning*, pages 2189–2200. PMLR, 2021.

N. Dagaev, B. D. Roads, X. Luo, D. N. Barry, K. R. Patil, and B. C. Love. A too-good-to-be-true prior to reduce shortcut reliance. *arXiv preprint arXiv:2102.06406*, 2021.

J. Devlin, M.-W. Chang, K. Lee, and K. Toutanova. Bert: Pre-training of deep bidirectional transformers for language understanding. *arXiv preprint arXiv:1810.04805*, 2018.

F. Ding, M. Hardt, J. Miller, and L. Schmidt. Retiring adult: New datasets for fair machine learning. In A. Beygelzimer, Y. Dauphin, P. Liang, and J. W. Vaughan, editors, *Advances in Neural Information Processing Systems*, 2021. URL `https://openreview.net/forum?id=bYi_2708mKK`.

J. C. Duchi, P. W. Glynn, and H. Namkoong. Statistics of robust optimization: A generalized empirical likelihood approach. *Mathematics of Operations Research*, 2021.

V. Feldman and C. Zhang. What neural networks memorize and why: Discovering the long tail via influence estimation. In *NeurIPS*, 2020.

A. Filos, P. Tigkas, R. McAllister, N. Rhinehart, S. Levine, and Y. Gal. Can autonomous vehicles identify, recover from, and adapt to distribution shifts? In *International Conference on Machine Learning*, pages 3145–3153. PMLR, 2020.

R. Geirhos, J.-H. Jacobsen, C. Michaelis, R. Zemel, W. Brendel, M. Bethge, and F. A. Wichmann. Shortcut learning in deep neural networks. *Nature Machine Intelligence*, 2(11):665–673, 2020.

K. Goel, A. Gu, Y. Li, and C. Re. Model patching: Closing the subgroup performance gap with data augmentation. In *International Conference on Learning Representations*, 2020.

I. Gulrajani and D. Lopez-Paz. In search of lost domain generalization. In *ICLR*. OpenReview.net, 2021.

G. Haixiang, L. Yijing, J. Shang, G. Mingyun, H. Yuanyue, and G. Bing. Learning from class-imbalanced data: Review of methods and applications. *Expert Systems with Applications*, 73:220–239, 2017.

Z. Han, Z. Liang, F. Yang, L. Liu, L. Li, Y. Bian, P. Zhao, B. Wu, C. Zhang, and J. Yao. Umix: Improving importance weighting for subpopulation shift via uncertainty-aware mixup. *arXiv preprint arXiv:2209.08928*, 2022.

M. Hardt, E. Price, and N. Srebro. Equality of opportunity in supervised learning. *Advances in Neural Information Processing Systems*, 29:3315–3323, 2016.

T. Hashimoto, M. Srivastava, H. Namkoong, and P. Liang. Fairness without demographics in repeated loss minimization. In *International Conference on Machine Learning*, pages 1929–1938. PMLR, 2018.

K. He, X. Zhang, S. Ren, and J. Sun. Deep residual learning for image recognition. In *Proceedings of the IEEE conference on computer vision and pattern recognition*, pages 770–778, 2016.

H. Ju, D. Li, and H. R. Zhang. Robust fine-tuning of deep neural networks with hessian-based generalization guarantees. In *International Conference on Machine Learning*, pages 10431–10461. PMLR, 2022.

B. Kang, S. Xie, M. Rohrbach, Z. Yan, A. Gordo, J. Feng, and Y. Kalantidis. Decoupling representation and classifier for long-tailed recognition. In *International Conference on Learning Representations*, 2019.

P. Kirichenko, P. Izmailov, and A. G. Wilson. Last layer re-training is sufficient for robustness to spurious correlations. *arXiv preprint arXiv:2204.02937*, 2022.

P. W. Koh, S. Sagawa, H. Marklund, S. M. Xie, M. Zhang, A. Balsubramani, W. Hu, M. Yasunaga, R. L. Phillips, I. Gao, et al. Wilds: A benchmark of in-the-wild distribution shifts. In *International Conference on Machine Learning*, pages 5637–5664. PMLR, 2021.

D. Krueger, E. Caballero, J.-H. Jacobsen, A. Zhang, J. Binas, D. Zhang, R. Le Priol, and A. Courville. Out-of-distribution generalization via risk extrapolation (rex). In *International Conference on Machine Learning*, pages 5815–5826. PMLR, 2021.

P. Lahoti, A. Beutel, J. Chen, K. Lee, F. Prost, N. Thain, X. Wang, and E. Chi. Fairness without demographics through adversarially reweighted learning. *Advances in neural information processing systems*, 33:728–740, 2020.

D. Levy, Y. Carmon, J. C. Duchi, and A. Sidford. Large-scale methods for distributionally robust optimization. *Advances in Neural Information Processing Systems*, 33:8847–8860, 2020.

D. Li and H. Zhang. Improved regularization and robustness for fine-tuning in neural networks. *Advances in Neural Information Processing Systems*, 34:27249–27262, 2021.

E. Z. Liu, B. Haghgoo, A. S. Chen, A. Raghunathan, P. W. Koh, S. Sagawa, P. Liang, and C. Finn. Just train twice: Improving group robustness without training group information. In *International Conference on Machine Learning*, pages 6781–6792. PMLR, 2021.

Z. Liu, P. Luo, X. Wang, and X. Tang. Deep learning face attributes in the wild. In *Proceedings of International Conference on Computer Vision (ICCV)*, December 2015.

Z. Liu, Z. Miao, X. Zhan, J. Wang, B. Gong, and S. X. Yu. Large-scale long-tailed recognition in an open world. In *Proceedings of the IEEE/CVF conference on computer vision and pattern recognition*, pages 2537–2546, 2019.

A. K. Menon, S. Jayasumana, A. S. Rawat, H. Jain, A. Veit, and S. Kumar. Long-tail learning via logit adjustment. In *International Conference on Learning Representations*, 2021a. URL `https://openreview.net/forum?id=37nvvqkCo5`.

A. K. Menon, A. S. Rawat, and S. Kumar. Overparameterisation and worst-case generalisation: friend or foe? In *International Conference on Learning Representations*, 2021b.

J. Nam, H. Cha, S. Ahn, J. Lee, and J. Shin. Learning from failure: Training debiased classifier from biased classifier. *arXiv preprint arXiv:2007.02561*, 2020.

J. Nam, J. Kim, J. Lee, and J. Shin. Spread spurious attribute: Improving worst-group accuracy with spurious attribute estimation. In *International Conference on Learning Representations*, 2022. URL `https://openreview.net/forum?id=_F9xpOrqyX9`.

L. Oakden-Rayner, J. Dunnmon, G. Carneiro, and C. Ré. Hidden stratification causes clinically meaningful failures in machine learning for medical imaging. In *Proceedings of the ACM conference on health, inference, and learning*, pages 151–159, 2020.

S. Sagawa, P. W. Koh, T. B. Hashimoto, and P. Liang. Distributionally robust neural networks for group shifts: On the importance of regularization for worst-case generalization. *International Conference of Learning Representation*, 2020a.

S. Sagawa, A. Raghunathan, P. W. Koh, and P. Liang. An investigation of why overparameterization exacerbates spurious correlations. In *International Conference on Machine Learning*, pages 8346–8356. PMLR, 2020b.

N. Sohoni, J. Dunnmon, G. Angus, A. Gu, and C. Ré. No subclass left behind: Fine-grained robustness in coarse-grained classification problems. *Advances in Neural Information Processing Systems*, 33, 2020.

M. Telgarsky. Deep learning theory lecture notes, 2021. URL `https://mjt.cs.illinois.edu/dlt/index.pdf`.

L. Van der Maaten and G. Hinton. Visualizing data using t-sne. *Journal of machine learning research*, 9(11), 2008.

P. Welinder, S. Branson, T. Mita, C. Wah, F. Schroff, S. Belongie, and P. Perona. Caltech-UCSD Birds 200. Technical Report CNS-TR-2010-001, California Institute of Technology, 2010.

A. Williams, N. Nangia, and S. R. Bowman. A broad-coverage challenge corpus for sentence understanding through inference. *arXiv preprint arXiv:1704.05426*, 2017.

H. Yao, Y. Wang, S. Li, L. Zhang, W. Liang, J. Zou, and C. Finn. Improving out-of-distribution robustness via selective augmentation. *arXiv preprint arXiv:2201.00299*, 2022.

C. Zhang, S. Bengio, M. Hardt, B. Recht, and O. Vinyals. Understanding deep learning requires rethinking generalization. In *ICLR*. OpenReview.net, 2017.

M. Zhang, N. S. Sohoni, H. R. Zhang, C. Finn, and C. Ré. Correct-n-contrast: A contrastive approach for improving robustness to spurious correlations. *ICML*, 2022.

Y. Zhang, B. Kang, B. Hooi, S. Yan, and J. Feng. Deep long-tailed learning: A survey. *arXiv preprint arXiv:2110.04596*, 2021.

B. Zhou, A. Lapedriza, A. Khosla, A. Oliva, and A. Torralba. Places: A 10 million image database for scene recognition. *IEEE Transactions on Pattern Analysis and Machine Intelligence*, 2017.

Table 7: Hyperparameters used in the experiments. The slash indicates the parameters used in the first phase (feature extractor) versus the second phase (classifier retraining).

	Waterbird	CelebA	MultiNLI	CivilComments
Learning Rate	$10^{-4}/10^{-4}$	$10^{-4}/10^{-4}$	$2 \times 10^{-5}/2 \times 10^{-5}$	$10^{-5}/10^{-5}$
ℓ_2 Regularization	$10^{-4}/10^{-4}$	$10^{-4}/10^{-4}$	0/0	$10^{-2}/0$
Number of Epochs	250/250	20/20	20/20	6/6

A Experimental Details

A.1 Infrastructure

We performed our experiments on 2 PCs with one NVIDIA RTX3070 and one NVIDIA RTX3090. Our implementation is built on top of the code base from Liu et al. (2021). Experimental data was collected with the help of Weights and Biases (Biewald, 2020).

A.2 Models

We use ResNet50 (He et al., 2016) with ImageNet initialization and batch-normalization for CelebA and Waterbird. We use pretrained BERT (Devlin et al., 2018) for MultiNLI and CivilComments. We use the original train-val-test split in all the datasets and report the *test* results. Cross-entropy is used as the base loss for all objectives. SGD with momentum 0.9 is used for the vision datasets while the AdamW optimizer with dropout and a fixed linearly-decaying learning rate is used for BERT. We use a batch size of 16 for CivilComments and 32 for the rest of the datasets. We do *not* use any additional data augmentation or learning rate scheduler in our results.

A.3 Hyperparameters

Table 7 contains the hyperparameters used in our experiments in Sections 4.2 and 4.1. Note that these are the standard parameters for obtaining an ERM model for these datasets as in previous works (Sagawa et al., 2020a; Liu et al., 2021). The only difference is that we train Waterbird and CelebA for slightly shorter epoch due to finding no further increase in validation accuracies after those epochs.

In our experiments, unless noted, we do not tune for any other hyperparameters. For the second phase of CivilComments, we do not use the default regularization but opt for 0 since the linear layer already has low capacity. However, adding further regularization does not seem to have much of an effect as in section C.1.

B Ablation studies: Obtaining a good feature extractor

B.1 Impact of The Feature Extractor's Algorithms

Here, we provide evidences that ERM trained models produce the best features for worst-group robustness. We conduct an experiment on Waterbird, where instead of using ERM to obtain a feature extractor, we perform GDRO and Reweighing instead on the first phase. The results are in table 8. While using reweighing or GDRO for the first phase defeats the purpose of reducing the amount of group-labels needed (whereas ERM doesn't need any), it is informative to examine the features alone.

Here, we see that even though ERM does not use group-labels, it provides the best features for robust classifier retraining on independent split.

B.2 Impact of Early Stopping and Validation Accuracies on The Feature Extractor

In this section, we present an ablation study of how different early stopping epoch (figure 4), average validation accuracy (figure 5 left), and worst-group accuracy (figure 5 right) of the initial ERM trained model (feature

Table 8: Effects of different methods for obtaining a feature extractor on test average accuracy and test worst-group accuracy (with ResNet50 on Waterbird).

Feature extractor via	Test Avg Acc	Test Wg Acc
Reweighing	90.1	88.8
GDRO	90.8	88.6
ERM	90.5	**90.2**

extractor) affect the GDRO retraining phase of CROIS. The results here are from performing CROIS with GDRO and $p = 0.30$ on Waterbird across a wide variety of epochs. Table 9 presents the full data generated for this section.

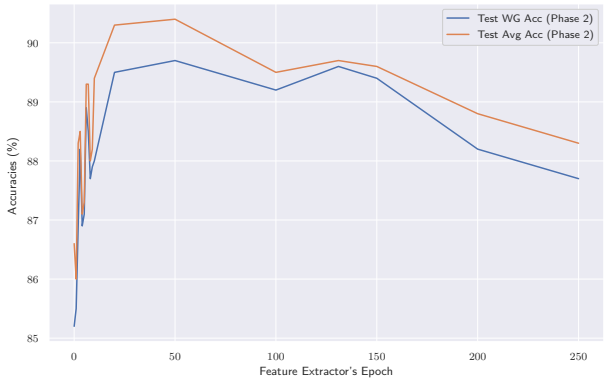

Figure 4: The effect of using different epochs for the feature extractor (phase 1) on classifier retraining's (phase 2) test accuracies.

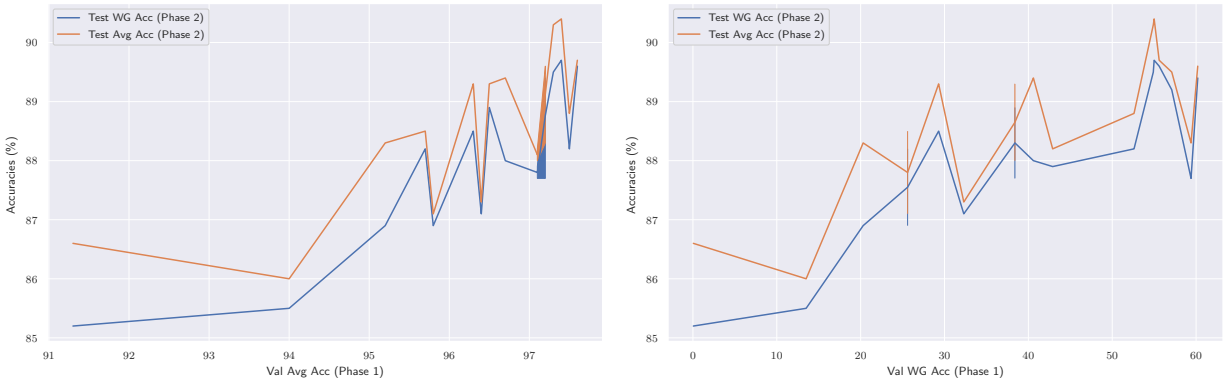

Figure 5: The effect of different *validation average accuracies* (**left**) and *validation worst-group accuracies* (**right**) from the feature extractor (phase 1) on classifier retraining's (phase 2) test accuracies.

C Hyperparameter tuning: CROIS vs. GDRO

C.1 Further hyperameter exploration on CROIS

In our paper, we have demonstrated CROIS's effectiveness even with just using the same hyperparameters as to train an ERM model. In this section, we present results for further additional parameter tuning on the

Table 9: CROIS with GDRO ($p = 0.30$) on Waterbird. Average (*Avg Acc*) and Worst-group (*Wg Acc*) Accuracies for various epochs of the feature extractor ("Phase 1") and the corresponding test accuracies for classifier retraining ("Phase 2"). While training for longer epochs seem to help with average and worst-group accuracy for phase 2, the benefit is small. Hence, simply selecting the best validation average accuracy model, row Epoch 131 and denoted *BEST* here, yields good enough features that simplify our training procedure and model selection criteria.

CROIS ($p = 0.3$)	Feature Extractor (Phase 1)		Classifier Retraining (Phase 2)			
Phase 1 Epoch	Val Avg	Val WG	Val Avg	Val WG	Test Avg	Test WG
0	91.3	0.05	87.8	85.6	86.6	85.2
1	94	13.5	88	87.6	86	85.5
2	95.2	20.3	89.6	88	88.3	86.9
3	95.7	25.6	90.1	88	88.5	88.2
4	95.8	25.6	88.9	88.2	87.1	86.9
5	96.4	32.3	89.2	88.7	87.3	87.1
6	96.5	38.4	90.5	88.7	89.3	88.9
7	96.3	29.3	90.6	88.7	89.3	88.5
8	97.1	38.4	90.1	89.3	88	87.7
9	97.1	42.9	90.4	89.9	88.2	87.9
10	96.7	40.6	91.2	90.2	89.4	88
20	97.3	54.9	91.4	91	90.3	89.5
50	97.4	55	**91.5**	91	**90.4**	**89.7**
100	97.2	57.1	90.5	90.2	89.5	89.2
131 (Best)	**97.6**	55.6	90.9	90.2	89.7	**89.6**
150	97.2	**60.2**	90.7	90.2	89.6	89.4
200	97.5	52.6	91	90.2	88.8	88.2
250	97.2	59.4	91	**90.4**	88.3	87.7

robust classifier retraining phase. These results provide empirical evidence for CROIS's potential as well as robustness to different hyperparameter setting.

ℓ_2 regularization. We investigate whether *additional* regularization would be helpful to classifier retraining with GDRO on CelebA (Table 10) and Waterbird. (Table 11) We further examine the effects of regularization on CivilComments (Table 12) to support our choice in Section A. For these experiments, we further run each setting acorss 3 random seeds to further investigate CROIS's sensitivity towards hyperparameters.

Table 10: Effects of ℓ_2 regularization on classifier retraining with GDRO on CelebA.

	$p = 0.50$		$p = 0.30$		$p = 0.10$	
ℓ_2 Reg.	Avg Acc	Wg Acc	Avg Acc	Wg Acc	Avg Acc	Wg Acc
1	91.6 (0.06)	87.4 (2.76)	90.9 (1.13)	88.4 (0.78)	91.2 (0.35)	90.0 (0.70)
10^{-2}	92.1 (0.32)	87.6 (1.56)	**91.8** (0.21)	87.5 (3.54)	92.0 (0.44)	88.3 (2.39)
10^{-4}	91.9 (0.35)	**88.2** (2.10)	91.3 (0.44)	**90.6** (0.95)	91.3 (0.36)	**90.3** (0.82)
0	**92.2** (0.25)	86.8 (2.30)	91.5 (0.07)	87.8 (3.96)	**92.1** (0.47)	88.1 (2.73)

Table 11: Effects of ℓ_2 regularization on classifier retraining with GDRO on Waterbird.

	$p = 0.50$		$p = 0.30$		$p = 0.10$	
ℓ_2 Reg.	Avg Acc	Wg Acc	Avg Acc	Wg Acc	Avg Acc	Wg Acc
1	89.6 (0.93)	88.9 (1.37)	**91.7** (0.44)	**89.8** (0.68)	94.5 (0.50)	85.8 (0.15)
10^{-2}	**90.4** (1.31)	89.3 (0.61)	90.6 (1.25)	89.2 (1.31)	95.1 (0.40)	86.3 (0.83)
10^{-4}	**90.4** (0.95)	**89.5** (0.59)	90.8 (0.35)	89.6 (1.15)	**95.4** (1.10)	83.5 (3.24)
0	89.8 (0.53)	89.3 (0.70)	90.6 (1.31)	89.1 (1.16)	95.1 (0.35)	**86.4** (0.90)

Table 12: Effects of ℓ_2 regularization on classifier retraining with GDRO on CivilComments.

	$p = 0.50$		$p = 0.30$		$p = 0.10$	
ℓ_2 Reg.	Avg Acc	Wg Acc	Avg Acc	Wg Acc	Avg Acc	Wg Acc
1	88.8 (1.30)	70.0 (1.63)	89.5 (0.35)	66.4 (1.99)	89.3 (1.69)	68.9 (2.64)
10^{-2}	89.4 (0.99)	70.6 (0.42)	89.5 (0.29)	68.5 (0.87)	88.6 (1.70)	**70.2** (1.63)
0	**89.5** (0.70)	**71.0** (1.50)	**89.7** (0.33)	**68.6** (1.53)	**89.5** (1.81)	68.7 (1.72)

Learning rate. We examine the effects of different learning rates on CROIS on CelebA and Waterbird in Table 13. Lower learning rate seems to be more beneficial.

Table 13: Effects of varying learning rate on CROIS $p = 0.30$ on CelebA and Waterbird. We fix ℓ_2 regularization to 10^{-4}.

	Learning rate	10^{-5}	10^{-4}	10^{-3}	10^{-2}	10^{-1}
CelebA	Average accuracy	**92.2**	91.4	91.2	90.1	91.2
	Worst-group accuracy	88.3	90	**90.3**	87.8	82.8
Waterbird	Average accuracy	89.7	90.6	**94.2**	93.2	93.9
	Worst-group accuracy	**89.5**	88.9	87.1	88.8	78.5

C.2 Sensitivity to model capacity: CROIS versus GDRO

In this section, we present a comparison between CROIS and GDRO test performance with different ℓ_2 regularization configuration on CelebA and Waterbird in Table 14. On CelebA, GDRO is quite sensitive to model capacity while it is less so on Waterbird. We note that GDRO fails to converge to a good stationary point when $\ell_2 = 1$ on CelebA (see Figure 3).

Table 14: Worst-group test accuracy for GDRO and CROIS ($p = 0.30$) with different ℓ_2 regularization.

	CelebA						Waterbird					
ℓ_2 reg.	0	10^{-4}	10^{-3}	10^{-3}	10^{-1}	1	0	10^{-4}	10^{-3}	10^{-3}	10^{-1}	1
GDRO	81.7	81.7	81.7	83.9	**87.8**	0.00	86.8	86.8	86.8	86.8	**87.1**	86.5
CROIS	90.6	**91.5**	90.0	90.0	90.3	90.0	90.3	**90.6**	90.6	90.6	90.0	88.2

D Further studies on classifier retraining

D.1 Impact of Robust Retraining on Independent Splits

In this section, we examine how robust retraining affects the model's prediction of D_U and D_L before and after robust classifier retraining on independent split (with $p = 0.30$). Tables 15 and 16 show the accuracy on

D_U and D_L for Waterbird and CelebA. The "Points changed" column indicates the number of points that the model changes prediction after robust retraining per group along with the total number of examples in that group (with percentage in parentheses). The worst-group is underlined in the tables.

Table 15: Model's prediction of D_U and D_L on Waterbird *before* robust retraining and *after* robust classifier retraining on independent split.

Waterbird ($p = 0.3$)	Accuracy on D_U			Accuracy on D_L		
	Before	After	Points changed	Before	After	Points changed
Avg Acc	100	94.5	184/3356 (5.48%)	96.4	89.6	162/1439 (11.3%)
Group 0 (73.0%)	100	<u>92.6</u>	180/2430 (7.41%)	99.6	<u>88.2</u>	122/1068 (11.4%)
Group 1 (3.84%)	100	99.3	1/141 (7.09%)	76.7	100	10/43 (23.3%)
Group 2 (1.17%)	100	100	0/38 (0.00%)	<u>44.4</u>	100	10/18 (55.6%)
Group 3 (22.0%)	100	99.6	3/747 (0.40%)	90.8	92.3	20/310 (6.45%)

Table 16: Model's prediction of D_U and D_L on CelebA before and after robust classifier retraining on independent split. RR means after Robust Retraining.

CelebA ($p = 0.30$)	Accuracy on D_U			Accuracy on D_L		
	Before	After	Points changed	Before	After	Points changed
Avg Acc	96.5	92.4	7537/113939 (6.61%)	95.6	92.0	3274/48831 (11.3%)
Group 0 (43.7%)	96.7	<u>91.7</u>	2609/50311 (5.19%)	95.8	<u>91.3</u>	1011/21318 (4.74%)
Group 1 (41.4%)	99.6	92.2	3489/46652 (7.48%)	99.6	92.2	1493/20222 (7.38%)
Group 2 (14.1%)	89.9	95.2	1000/16012 (6.25%)	86.8	93.7	517/6868 (7.53%)
Group 3 (0.87%)	<u>46.3</u>	91.8	439/964 (45.4%)	<u>35.5</u>	95.3	253/423 (59.8%)

Interestingly, after robust retraining, the worst-group almost always switches from the minority group to the majority group regardless of the data split.

D.2 The Importance of Minority Examples: Subsampled Retraining

As alluded to in Section 4.2, group-imbalance seems to play an important role in the robust performance of CROIS. To further demonstrate this point, we consider how CROIS performs when the second phase is subsampled versus when it is allowed additional non-minority examples.

Table 17: Performance of CROIS when retraining is on a subsampled split versus the full split. Subsampling the split doesn't seem to impact CROIS's performance, indicating the importance of the availability of minority examples.

Dataset (minority group size, fraction)	Subsampled retraining		Full retraining	
	Avg Acc	Wg Acc	Avg Acc	Wg Acc
CelebA ($n = 423$, 0.87%)	90.6	89.7	91.9	88.9
Waterbird ($n = 18$, 1.2%)	91.3	87.6	90.3	88.9

As the result in Table 17 shows, there isn't a significant difference between the two sampling strategies, suggesting that the availability of minority group examples plays an important role in robust classifier retraining.

Table 18: Experimental results for the setting when only group labels from the validation set are used. Results for C-DRO (CVaR DRO), LfF, EIIL, JTT and SSA are from Nam et al. (2022). Results for UMIX are from Han et al. (2022). Results for CnC are from Zhang et al. (2022). The numbers in parentheses denote one standard deviation from the mean across 3 random seeds.

	Waterbird		CelebA		MultiNLI		CivilComments	
Method	Avg Acc	Wg Acc	Avg Acc	Wg Acc	Avg Acc	Wg Acc	Avg Acc	Wg Acc
C-DRO	96.0	75.9	82.5	64.4	82.0	68.0	92.5	60.5
LfF	91.2	78.0	85.1	77.2	80.8	70.2	92.5	58.8
EIIL	91.2	78.0	85.1	77.2	80.8	70.2	92.5	58.8
JTT	93.9	86.7	88.0	88.1	78.6	72.6	91.1	69.3
UMIX	93.0 (0.5)	90.0 (1.1)	90.1 (0.4)	85.3 (4.1)	N/A	N/A	90.6 (0.4)	70.1 (0.9)
CnC	90.9 (0.1)	88.5 (0.3)	89.9 (0.9)	88.8 (0.9)	N/A	N/A	81.7 (0.5)	68.9 (2.1)
SSA	92.2 (0.87)	89.0 (0.55)	92.8 (0.11)	**89.8** (1.28)	79.9 (0.87)	76.6 (0.66)	88.2 (1.95)	69.9 (2.02)
CROIS	92.1 (0.29)	**90.9** (0.12)	91.6 (0.61)	88.5 (0.87)	81.4 (0.06)	**77.4** (1.21)	90.6 (0.20)	**70.3** (0.34)

Table 19: Additional comparison where group labels from the training set are available. Results for LISA are taken from Yao et al. (2022). Results for CAMEL are taken from Goel et al. (2020).

	Waterbird		CelebA		MultiNLI		CivilComments	
Method	Avg Acc	Wg Acc	Avg Acc	Wg Acc	Avg Acc	Wg Acc	Avg Acc	Wg Acc
ERM	96.9	69.8	95.6	44.4	82.8	66.0	92.1	63.2
GDRO	93.2†	86.0†	91.8†	88.3†	81.4†	77.7†	89.6 (0.23)	70.5 (2.10)
LISA	91.8 (0.3)	89.2 (0.6)	92.4 (0.4)	89.3 (1.1)	N/A	N/A	89.2 (0.9)	**72.6** (0.1)
CAMEL	90.9 (0.9)	89.1 (0.4)	N/A	N/A	N/A	N/A	N/A	N/A
CROIS' p – group-labeled fraction used for retraining (with $1-p$ unlabeled fraction for the ERM phase)								
0.10	95.4 (1.10)	83.5 (3.24)	91.3 (0.36)	90.3 (0.82)	80.8 (0.51)	75.3 (2.06)	89.5 (1.81)	68.7 (1.72)
0.30	90.8 (0.35)	**89.6** (1.15)	91.3 (0.44)	**90.6** (0.95)	80.0 (0.31)	**77.9** (0.17)	89.7 (0.33)	68.6 (1.53)

E Additional Comparison

We provide additional baselines for comparison in the Tables below.

E.1 Additional baselines for group labels from only the validation set

Baselines. In Table 18, we compare CROIS against JTT (Liu et al., 2021) and SSA (Nam et al., 2022), as well as additional baselines like CVaR DRO (Levy et al., 2020), LfF (Nam et al., 2020), EIIL (Creager et al., 2021), CnC (Zhang et al., 2022) and UMIX (Han et al., 2022). There, we report the mean and one standard deviation of the Test Average (*Avg Acc*) and Worst-Group Accuracy (*Wg Acc*) across three random seeds.

E.2 Additional baselines for group labels from training set

In the setting where group labels are available from the training set, we compare our method against additional baselines like LISA (Yao et al., 2022).

F Fraction of the validation set implementation details from Section 4.1

Following the setup in Section 4.1 and the setup as in Liu et al. (2021); Nam et al. (2022), we further reduce the validation set to only a small fraction, 5%, 10%, and 20%. We investigate CROIS's performance in this very few group-labels setting across CelebA and Waterbird in Section 4.1. We note that the highly reduced sample size poses new challenge and makes it harder to simply reuse the default parameters.

- **Tuning ℓ_2 regularization:** When using so little data, overfitting can become a bigger problem, even when just training a low-capacity linear classifier. Hence, we tune for higher values for ℓ_2 regularization across $\{10^{-4}, 10^{-2}, 1, 10\}$.
- **Tuning learning rate:** We also tune the learning rate across $\{10^{-5}, 10^{-4}, 10^{-3}, 10^{-2}\}$ instead of simply reusing default parameters.
- **The use of group-labels and model selection:** Since the amount of examples for classifier retraining is now significantly reduced, it might be wasteful to further split our available group-labels for validation. Instead, we use all the available group-labels for robust classifier retraining and perform model selection in the second phase via the *train worst-group accuracy*. The low capacity linear layer and higher ℓ_2 regularization allows us to avoid overfitting when performing model selection this way. The feature extractor from the first phase is selected via the best average accuracy on the full group-unlabeled validation set.
- **Smaller batch size:** Since GDRO requires group-balanced sampling, a batch size greater than the number of examples in a certain group would cause duplicate sampling of the minority-group examples in the same step, artificially increasing the weight for that group. We further tune for batch sizes across a grid of powers of 2 less than the smallest group or the default batch size (e.g. we search across $\{4, 8, 16\}$ if the size of the smallest group is 17).

In Table 2, we present the results for CROIS with the above modifications and compare it to CROIS and JTT. There, robust retraining for CelebA is performed with an ℓ_2 regularization of 0.1, batch size of 8 and learning rate 10^{-5}. For Waterbird, we found that batch size 8, weight decay 1, and learning rate 10^{-5} are best for 20% and 10% reduction. For 5% reduction, we further reduce the batch size to 4 (since the minority group only has 7 examples) and increase the weight decay to 10.

The results shows that CROIS maintains its robustness performance even at greatly reduced group-labels. This implies that even a few (minority) examples can help debias the final layer classifier with proper configurations.

G Omitted Proofs from Section 5

Proof of Theorem 1. We look to apply the standard Radamacher Complexity generalization bound on the function class $\mathcal{F}_{|S}$. Recall that the standard Radamacher Complexity generalization bound (see for example Theorem 13.1 in Telgarsky (2021) and references therein) gives that for a function class $\mathcal{F}$ where for each $f \in \mathcal{F}$, $f \in [a, b]$, and dataset $S = \{z_1, z_2, \ldots, z_n\}$ with n i.i.d. samples from some population distribution, we have that with probability at least $1 - \delta$

$$\sup_{f \in \mathcal{F}} \mathbb{E}\left[f(Z)\right] - \frac{1}{n}\sum_{i=1}^{n} f(z_i) \leq \frac{2}{n} R(\mathcal{F}_{|S}) + 3\,(b-a)\sqrt{\frac{\ln\left(2/\delta\right)}{2n}},$$

where for Radamacher random variables $\epsilon_i \in \{-1, +1\}$, we have that

$$R(\mathcal{F}_{|S}) := \mathbb{E}_{\epsilon}\left[\sup_{f \in \mathcal{F}} \sum_{i=1}^{n} \epsilon_i f(z_i)\right]$$

is the Radamacher complexity of $\mathcal{F}$. Now, we simply bound the Radamacher Complexity of $\mathcal{F}_{|S}$ (Theorem 14.1 of Telgarsky (2021)):

$$R(\mathcal{F}_{|S}) \leq \|X\|_{2,\infty} \left(2\rho B\right)^L \sqrt{2\ln\left(d\right)}.$$

This gives us the generalization bound. □

Proof of Theorem 2. If we collect samples $x_1, \ldots, x_n$ into rows of $X \in \mathcal{X}^{n \times d}$, then Theorem 13.3 from Telgarsky (2021) gives that

$$R\left(\mathcal{F}_{|S}\right) \leq B \cdot \|X\|_F.$$

Similarly, if we collect samples of S_i into rows $X^{(i)} \in \mathcal{X}^{n_i \times d}$, then we have

$$R\left(\mathcal{F}_{|S_i}\right) \leq B \cdot \left\|X^{(i)}\right\|_F.$$

Then combining with Radamacher-complexity generalization bound gives that with probability at least $1-\delta$

$$\sup_{f \in \mathcal{F}} \mathbb{E}\left[f(Z)\right] - \frac{1}{n}\sum_{i=1}^{n} f(z_i) \leq \frac{2}{n} B \cdot \|X\|_F + 3\left(\ln(2) + B\right)\sqrt{\frac{\ln\left(2/\delta\right)}{2n}},$$

where the range of $f \in \mathcal{F}_{|S}$ is $l(\langle w, xy\rangle) \leq \ln(2) + \langle w, xy\rangle \leq \ln(2) + B$. For a group $i \in G$ with training samples $X^{(i)}$ and f being linear classifiers with max norm B, we have that with probability at least $1-\delta$

$$\sup_{f \in \mathcal{F}} \mathbb{E}_{(X,Y)|g(X)=i}\left[\ell(f(X), Y)\right] - \frac{1}{n_i}\sum_{j} \ell(f(x_j), y_j) \leq \frac{2}{n_i} B \cdot \left\|X^{(i)}\right\|_F + 3\left(\ln(2) + B\right)\sqrt{\frac{\ln\left(2/\delta\right)}{2n_i}}.$$

Now, letting $\hat{R}_i(f) := \frac{1}{n_i}\sum_j \ell(f(x_j), y_j)$ and $R_i(f) := \mathbb{E}_{(X,Y)|g(X)=i}\left[\ell(f(X), Y)\right]$ denotes the empirical and population group loss of f and taking a union bound over all the groups, we have that with probability at least $1-\delta$

$$\max_{i \in G} \sup_{f \in \mathcal{F}} R_i(f) - \hat{R}_i(f) \leq \max_{i \in G} \frac{2}{n_i} B \cdot \left\|X^{(i)}\right\|_F + 3\left(\ln(2) + B\right)\sqrt{\frac{\ln\left(2G/\delta\right)}{2n_i}}.$$

Since the RHS is finite, we can swap the max and sup on the LHS and we have

$$\sup_{f \in \mathcal{F}} \underbrace{\max_{i \in G} R_i(f) - \hat{R}_i(f)}_{\text{WG generalization error}} \leq \max_{i \in G} \frac{2}{n_i} B \cdot \left\|X^{(i)}\right\|_F + 3\left(\ln(2) + B\right)\sqrt{\frac{\ln\left(2G/\delta\right)}{2n_i}}.$$

□

H Implications and takeaways

Comparison to standard pretraining and finetuning As mentioned in the related works section as well as during the discussion of the motivation for our method, pretraining and then finetuning is a now well-known and established strategy in many domains. Our work differs the most significantly from this standard strategy through:

1. The use of independent splits: Traditional pretraining and finetuning reuses the dataset for both phase with the possibility of additional labels (contrastive learning, long-tail learning, etc.). We have demonstrated through extensive experiments the importance of independent split for classifier retraining to work well for the group robust setting.
2. The use of a group robust algorithm for finetuning: We mainly utilize GDRO for our finetuning phase while most other works in finetuning make use of simpler strategy for finetuning like reweighing or subsampling. We demonstrated in our experiments that GDRO yields the best robust performance over other more common methods.

Our work provides evidences that the features of ERM trained DNNs are rich enough to solve the group-shift problem (when an abundant amount of group labels is available to retrain the classifier) and one of the major reasons for poor worst-group performance of an ERM trained DNN is within its classifier layer. We then further demonstrate that even a few group labels can sufficiently "fix" the classifier to achieve better group-robust performance.

This knowledge can potentially be useful towards solving the seemingly much harder group-agnostic setting (where no group label is available) by allowing the practitioner to focus on obtaining a robust classifier given

an ERM trained feature extractor. Our experiments further show that reasonable robustness can be achieved with relatively few group-labels (that are not used to obtain the feature extractor), which makes the problem seem closer in reach.